J Geophys (1986) 60:186–198

Journal of Geophysics

Spatial and temporal characteristics of impulsive structure of magnetospheric substorm

V.A. Sergeev[1], R.J. Pellinen[2], T. Bösinger[3], W. Baumjohann[4], P. Stauning[5], A.T.Y. Lui[6]

[1] University of Leningrad, Institute of Physics, 198904 Leningrad, USSR
[2] Finnish Meteorological Institute, Department of Geophysics, Box 503, SF-00101 Helsinki 10, Finland
[3] University of Oulu, Department of Physics, SF-90570 Oulu 57, Finland
[4] Max-Planck-Institut für Physik und Astrophysik, Institut für Extraterrestrische Physik, D-8046 Garching, Federal Republic of Germany
[5] Danish Meteorological Institute, Division of Geophysics, DK-2800 Lyngby, Denmark
[6] Johns Hopkins University, Applied Physics Laboratory, Laurel, MD 20707, USA

Abstract. At least a dozen well-defined activations were recorded with high spatial resolution during the first 25 min of a substorm commencing at 1959 UT on 3 March 1976. The activations were determined by Pi1 and 2-type magnetic pulsations, magnetic variations and cosmic noise absorption. The activations exhibited differences in intensity, spatial extent and the accompanied auroral behaviour. In all cases but one an impulsive counterclockwise differential equivalent current vortex was observed superimposed on the continuously growing westward electrojet. The high-energy particle precipitation reached its maximum in these vortex regions. In cases where the activations observed on the ground occurred close to the footpoint of the IMP-J satellite, it registered simultaneously (within 2 min) burst-like enhancements of the high-energy particle fluxes. The satellite was at these times 37 R_E away from the earth in the plasma sheet boundary layer.

Large, practically isotropic high-energy electron fluxes detected at the satellite during the substorm expansion suggested the existence of a large-scale magnetic loop structure in the far magnetotail. The results give evidence of a time-varying dissipation process operating in an impulsive manner in separate regions of the plasma sheet (within a few R_E). According to the magnetic variations at mid-latitude, the intensity of the cross-tail current disruption (or the substorm current wedge) does not respond to these activations in the same impulsive manner, but seems to integrate their effects.

Key words: Magnetospheric substorm – Microsubstorm – Substorm current wedge – Pi2 and Pi1B pulsation – Auroral behaviour – Plasmoid – Magnetotail acceleration

Introduction

It is commonly known that the development of a magnetospheric substorm process can occur in several different ways. Concepts such as the "classical" substorm (Akasofu, 1968), the convection bay (Sergeev, 1977; Pytte et al., 1978), the multiple onset substorm (Wiens and Rostoker, 1975; Pytte et al., 1976b) and the microsubstorm (Sergeev, 1974) have been introduced to classify the different modes of substorm-related processes. In order to understand the basic physics involved in the dissipation mechanisms, it has turned out to be necessary to introduce one more concept; an "elementary event", i.e. one which does not contain any further temporal or spatial fine structure. It is assumed that all impulsive magnetospheric dissipation processes, even if they show extreme complexity and variability, are made up of a series of these elementary events. It is the main task of this paper to investigate, both on the ground and in space, the temporal and spatial scales of these elementary events and to compare the present results with existing theoretical models.

In the past, two different time-scales have been identified in the fine structure of ground-based substorm data. The first, 5–15 min, represents the interval between substorm intensifications (or microsubstorms). The second, 1 min, characterizes details in the temporal fine structure of substorm intensifications. What is meant by substorm intensification is well documented in literature (Sergeev, 1974; Wiens and Rostoker, 1975; Vorobjev and Rezhenov, 1973; Pytte et al., 1976a, b and c). If the duration of the Pi2 train and/or deflection in mid-latitude and auroral-zone magnetic bays are taken as a time measure of the substorm intensification, one can say that a substorm intensification lasts typically some 5 min. Within this time interval burst-like enhancements can usually be noticed. They represent a fine structure of the substorm intensification. It was discovered and described first by Sergeev et al. (1978), Sergeev and Yahnin (1979), and Yahnin et al. (1983). It can be added that the substorm analyses underlying the document of the Victoria Workshop (Rostoker et al., 1980) were not detailed enough in the temporal and spatial evolution of substorm intensifications for a description of a substructure of the intensification. This substructure constitutes – what we have called – elementary events. In other words, a sequence of elementary events forms a substorm intensification (microsubstorm). This paper domonstrates (once again) the coexistence of the different time scales characterizing the substorm development.

Short-lived, localized features have been reported to occur in the plasma sheet (PS) during substorm processes (cf. Aggson et al., 1977; Krimigis and Sarris, 1979; Coroniti et al., 1980), although it is impossible to separate temporal and spatial effects by means of single-satellite measurements. Multiple-satellite observations may be useful in this

Offprint requests to: R.J. Pellinen

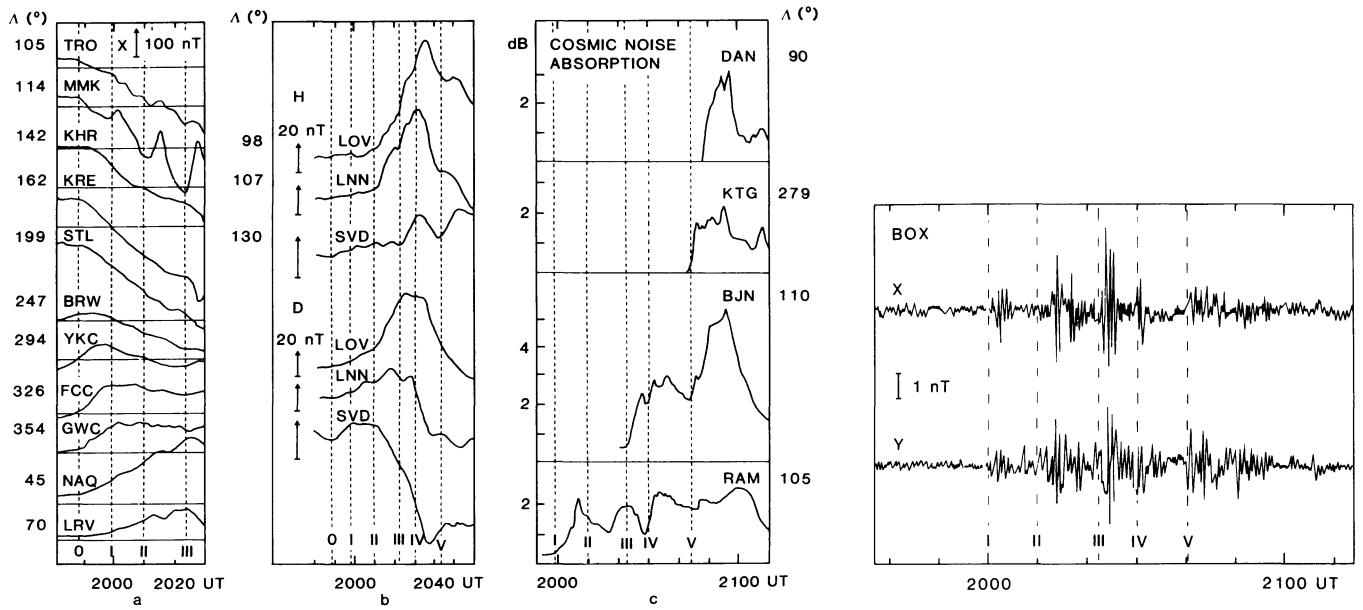

Fig. 1a–d. General characteristics of the substorm event starting at 1959 UT on 3 March 1976. **a** *H*-component variations at auroral-zone stations around the northern hemisphere; **b** Mid-latitude magnetic variations; **c** Cosmic noise absorption; **d** Pi2 recordings at Borok. Five microsubstorms (I–V) are indicated by *broken vertical lines*

respect, but have until now only rarely been reported. The problem of spatial and temporal separation may partially be overcome by forming a global picture of substorm development by means of ground-based data and by comparing the spatial and temporal details on the ground with satellite recordings.

A correlation study of irregular pulsations on the ground and processes in the PS is carried out in an accompanying paper (Sergeev et al., 1986, referred to in the following as paper I). One important conclusion of paper I is that the time scale of 1–3 min represents an "elementary" length for an impulsive substorm process in the PS. In this paper we deal mainly with the spatial aspects of the elementary events, studying their localized character on the ground and impulsive response near the upper boundary of the remote PS.

The present investigation concerns a substorm that was unusually well suited for such detailed treatment. The expansion phase commenced at 1959 UT on 3 March 1976, and the region of impulsive expansion processes in the ionosphere was within the field of view of the Scandinavian geophysical network for the next 25 min. The IMP-J satellite was located in the far PS on the field line mapping into the same magnetic local time (MLT) sector where the ground-based recordings were made. A dozen impulsive elementary events were detected within the first 25 min, most of them with a clear ground-PS correlation.

Description of the event

The event under consideration is one of the substorm periods of 3 March 1976 which have already been investigated by a working group of scientists. An extensive set of data has been gathered from both permanent and temporary ground observatories and from the IMP-J satellite. Corresponding data reviews have been published by Sergeev et al. (1981) and Mishin et al. (1982). Figure 1 presents results of ground-based observations of various types. According to all the data obtained both on the ground and in the magnetotail, the substorm onset took place at 1959 UT over Kevo (see Fig. 5), approximately at 66° corrected geomagnetic latitude (CG Lat, Tsyganenko, 1979) within the sector 110°–115° CG Long (~23.0 MLT). We are primarily interested in the 25-min period after the onset, since the auroral expansion subsequently moved outside the field of view of the Scandinavian network and there is a gap in the satellite data after 2025 UT.

The substorm started at the end of the recovery phase of a preceding strong substorm that commenced at 1715 UT. Both the polar-cap (data not shown here) and auroral-zone magnetic data show an intensification in the convection-driven twin-vortex DP2 current system after 1948 UT (Fig. 1a). According to these data and those from other stations published in Mishin et al. (1982), a monotonous increase in convection-related auroral electrojets (AEJ) and their equatorward expansion continued at least during the period under investigation. Both the oval expansion and the increase in magnetic-field magnitude at IMP-J in the magnetotail are evidence of a growing tail current.

According to the mid-latitude pulsation data in Fig. 1d, at least five well-defined Pi2 trains occurred during the expansion phase. As usual, these five microsubstorms are pronounced both in the mid-latitude magnetic variations (Fig. 1b) and in the cosmic noise absorption (CNA) data from the auroral zone (Fig. 1c). Only the first three lie within the period under consideration.

No significant Pi activity or CNA enhancement was observed during the entire event at two Antarctic stations, Molodeznaya and Syowa (approximately at 67° CG Lat and 70° CG Long). The riometer data from this longitude sector (Sergeev et al., 1981) suggest that expansion-associated increases in CNA appeared at higher latitudes only after 2045 UT (Fig. 1c). Hence, the western edge of the substorm expansion is estimated to have been at 80°–90° CG Long (~21.5 MLT) until 2030 UT.

To the east, at 145°–160° CG Long, both magnetic and

Table 1. Geographic and corrected geomagnetic coordinates (Tsyganenko, 1979) of the permanent or temporary stations from which data are used

Station	Symbol	Geographic coordinates		Corrected geomagnetic	
		Latitude	Longitude	Latitude	Longitude
Barrow	BRW	71°	203°	70°	247°
Bjørnøya (Bear Island)	BJN	75	19	71	110
Borok	BOX	58	39	54	114
Danmarkshavn	DAN	77	341	77	90
Fort Churchill	FCC	59	266	70	326
Great Whale River	GWC	55	282	67	354
Kaliningrad	KNG	55	21	50	98
Kap Tobin	KTG	70	238	76	279
Kerguelen	KGL	−49	70	−59	121
Kevo	KEV	70	27	66	111
Kharasovey	KHR	65	72	66	142
Kiruna	KIR	68	20	64	107
Kresty	KRE	72	88	66	162
Leirvogur	LRV	64	338	66	70
Leningrad	LNN	60	31	55	107
Loparskaya	MMK	68	33	65	114
Lovozero	LOZ	68	35	64	116
Lovö	LOV	59	18	56	98
Muonio	MUO	68	24	64	108
Narssarssuaq	NAQ	61	315	67	45
Port Alfred	CZT	−46	52	−53	105
Ramfjord	RAM	70	19	66	105
Sokankylä	SOD	67	27	63	109
Stolbovoy	STL	74	133	68	199
Sverdlovsk	SVD	57	61	52	134
Tbilisi	TFS	42	45	36	117
Tromsø	TRO	70	19	67	105
Yellowknife	YKC	62	245	70	294

photometric data (not shown here) fail to show any expansion-associated signatures during the period concerned (Sergeev et al., 1981; Mishin et al., 1982). The mid-latitude data in Fig. 1b lead us to infer that before 2023 UT the eastern edge of the substorm current wedge (SCW) was located west of 130° CG Long. Only during the third microsubstorm (III) did the *H*-component at SVD start to rise, indicating that the SCW had extended beyond 130° CG Long (~00.0 MLT).

It was only at 2023 UT that the CNA started to increase at BJN (Fig. 1c). Thus before this time the active region was restricted in both latitude (within 65°–69° CG Lat) and longitude (between 21.5–00.0 MLT), causing the auroral activity to remain in the field of view of the Scandinavian observatories during most of the period 1959–2025 UT.

The observation sites are listed in Table 1. Auroras were recorded by all-sky cameras (ASC) at KEV, MUO, SOD and MMK (Loparskaya) at a speed of 1 frame/min. CNA was monitored by a riometer network (described in Ranta et al., 1981) with a time resolution of about 0.5 min (chart speeds 60 or 76 mm/h). Pulsation recordings (frequency range 0.1–2 Hz) were made at Sodankylä and Nurmijärvi (details in Bösinger et al., 1981). Only two chains (~104° and 107° CG Long) of the Scandinavian Magnetometer Array (SMA, Küppers et al., 1979) were in operation; time resolution, 10 s. In addition, sensitive rapid-run magnetograms (90 mm/h) were available from LOZ. Mid-latitude magnetic data (resolution ≤1 min) were collected from a longitudinal chain of observatories (105°–133° CG Long). Mid-latitude induction magnetometer data (0.01–0.2 Hz) were obtained from a meridional chain of stations (36°–64° CG Lat).

The IMP-J satellite performed measurements near the upper boundary of the plasma sheet at a distance of 37 R_E from the earth. Its ionospheric projection along the magnetic field line is estimated to be at 117° CG Long, just at the eastern border of the Scandinavian network (details in later section).

Temporal development of the impulsive events

Burst-like Pi1 pulsations (Pi1B) recorded at auroral and subauroral latitudes show a clear response to strong or weak, wide or localized substorm activations, if the recordings are carried out in the MLT sector of the activation (Bösinger et al., 1981; Yahnin et al., 1983). In the present study, Pi1Bs provide the most accurate definition of the temporal sequence of the impulsive activations.

Intensity variations of Pi1 pulsations in a few frequency bands (Fig. 2a) synchronously display a large number of bursts. Bursts that are well separated and distinct through all frequency bands are indicated by dotted vertical lines and letters. Similar impulsive Pi1B structures appear both at Sodankylä (Fig. 2a) and at Nurmijärvi (located 800 km further south).

According to the results reported in Sergeev et al. (1978) and its supporting verifications in Sergeev (1981) and Yahnin et al. (1983), similar impulsive activations are seen even at mid-latitudes in the form of sudden changes in the characteristics of Pi2 pulsations (intensity and phase).

In Fig. 2b 1-min time intervals are marked by a shaded vertical band laid across the Pi2 registrations of one auroral-zone (LOZ) and three mid-latitude (BOX, KNG and TFS) stations. Within these time intervals at least four instances of Pi2 onsets and/or sudden changes in the Pi2 waveform indicating activations can be recognized in the seven Pi2 registrations displayed. A length of 1 min for the time intervals was chosen because it is representative of the time accuracy of the method in question (average period of Pi2s, some 60 s).

The Pi2 data of Fig. 2b reveal some additional activations of which the most significant ones are marked as A′, F′, G′ and I′. At least two of these (A′ and G′) correspond to additional strong spikes within the Pi1Bs in Fig. 2a.

Response of other ground-based phenomena to the impulses

Energetic electron precipitation and equivalent currents in the ionosphere

Figure 3 (upper panel) demonstrates well both the impulsive variations and the spatial changes in the high-energy electron precipitation patterns. The auroral break-up at 1959 UT (A) started at ~66° CG Lat and significant auroral activity was confined between 65° and 69° CG Lat until 2023 UT (I). Most of the active auroras throughout the period were within the riometer beams of KEV and RAM, which are located 270 km apart on the same 66.6° CG Lat. Hence the data from these two stations

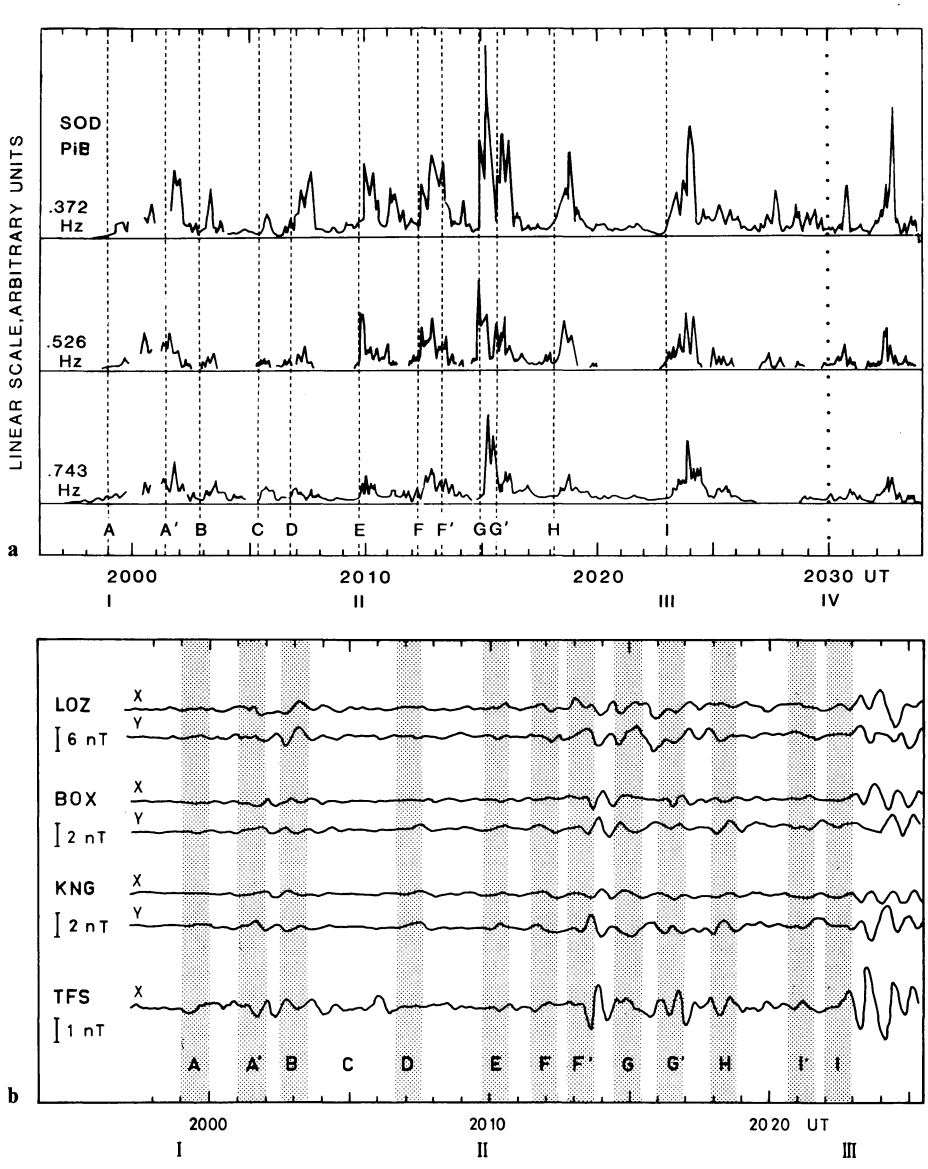

Fig. 2. a PiB amplitudes in different frequency channels at Sodankylä; **b** Pi2 recordings from the auroral zone (LOZ) to mid-latitude (TFS) in the longitudinal sector of the auroral expansion. The *vertical shaded bands* (A–I) indicate impulsive activations

(Fig. 3) demonstrate the changes in energetic precipitation pattern during the time interval under consideration.

There is a striking difference in CNA behaviour between KEV and RAM. In the east (KEV), distinct rises in CNA are seen in response to impulses A and G′ (with less confidence for F′); while in the west (RAM), the responses to the same impulses are absent or negligible. Conversely, responses to impulses B, C, D and H are only observed in the west. Thus, most of the impulses A–H are associated with an enhancement in the energetic electron precipitation in very localized MLT sectors. Impulse I gives no immediate response at these locations, but results in a sharp onset of CNA at BJN (71° CG Lat, Fig. 1c).

Data from three magnetometer stations (Fig. 3, lower panels), aligned along 64° CG Lat within the 104°–114° CG Long sector, demonstrate the response of equivalent currents. At 1950 UT the magnetic *A* and *B* components (directed approximately northwards and eastwards; for an exact definition, see Küppers et al., 1979) are almost at the quiet-time level (within 10–20 nT) before the onset, the *A* components decreasing monotonically until 1959 UT, this being most effective at the easternmost station, LOZ. The substorm started at 1959 UT in the sector 108°–115° CG Long, eastwards of MUO, obviously in the region of a westward auroral electrojet (AEJ). We can infer from Fig. 1a that during the period concerned here the monotonical growth of the convection-associated westward AEJ continued in the morning sector of the oval, and apparently also within the expansion sector. The latter tendency is indicated by the broken lines in Fig. 3, which also serve (at least in a qualitative sense) as reference lines for the impulse-associated responses.

Figure 3 shows that the clearest responses appear in the *A* component, in the form of sudden increases associated with most of the impulses A–I. The significance of this observation is underlined by the similarity of the magnetic field behaviour at MUO and LOZ to the CNA development at KEV (located approximately at the mid-point between the two magnetometer sites). The details of the magnetic-field trends at KIR, MUO and LOZ differ, however, suggesting spatial changes in the active region between the impulses. Hence, information from the entire SMA seems to be of utmost importance for this purpose.

It may be concluded from the discussion above that

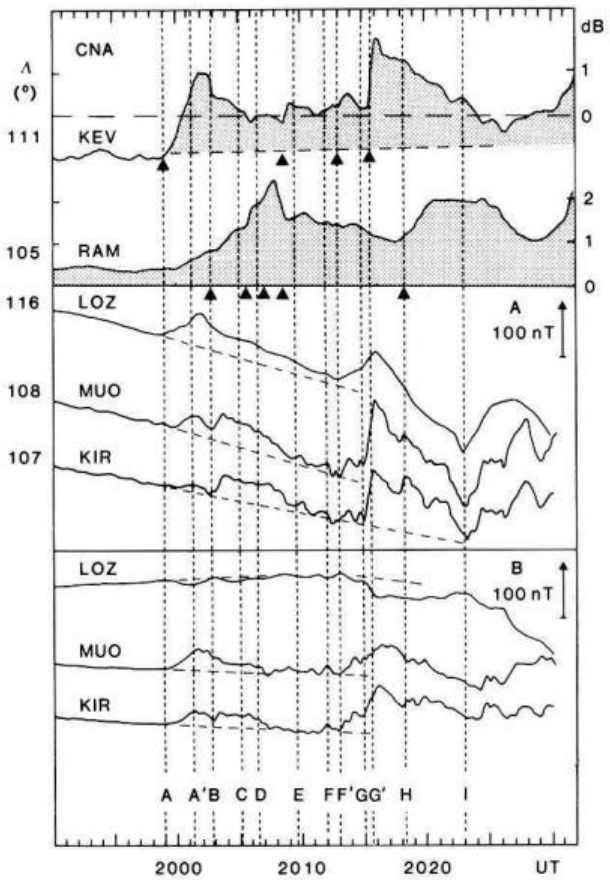

Fig. 3. Changes in cosmic noise absorption (*top panel*) and magnetic field variations (*middle and bottom panel*) at a longitudinal chain of stations. The *vertical broken lines* are the same as in Fig. 2, *triangles* denote onsets of CNA enhancements

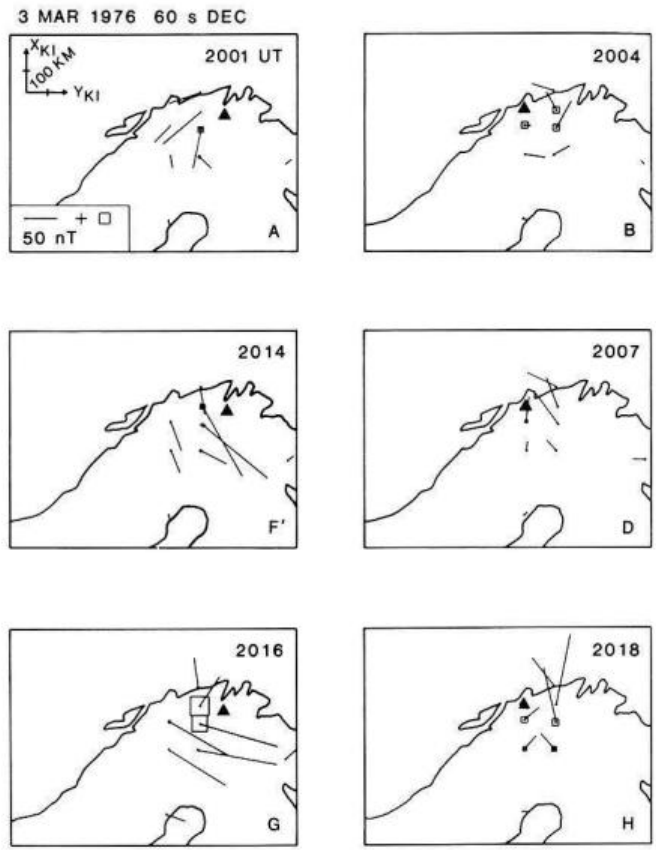

Fig. 4. Differential equivalent current patterns building up during 1 min around the activations A, B, D, F′, G and H. CNA enhancement occurs at Kevo (*triangle*) in the left-hand column, and at Ramfjord (*triangle*) in the right-hand column

the magnetic variations superimposed on the monotonically growing convection background are in accordance with the sequence of impulses reported in Fig. 2. Hence the method of differential equivalent current (DEC) analysis introduced by Untiedt et al. (1978) and Opgenoorth et al. (1980), showing the relative changes in current patterns after each impulse, seems to be fairly convenient here.

As shown above, the impulses can be separated roughly into two different groups (the western and eastern ones), depending on the appearance of the CNA increases at RAM or KEV. Figure 4 clearly demonstrates that the DEC patterns are similar within each group, while there are differences between the groups. Assuming that the DEC patterns for each impulse are similar within the observation site covering the active region, we can combine the DEC patterns of both groups. This results in a counterclockwise equivalent current vortex for each case centred at the peak precipitation area for high-energy electrons.

Our results exhibit a clear response of both equivalent currents and CNA behaviour to individual impulses. The impulse-induced patterns seem to be short-lived. After a rapid formation phase (~1 min), the vortex tends to fade within 2–3 min. Similar features are reported in Yahnin et al. (1983). There are also some similarities in the time and amplitude structures of the vortices and mid-latitude Pi2s (cf. Fig. 2b), in that a good correlation can be found in the case of B, D, F′, G and H, suggesting a close relationship between their source mechanisms.

Intensity, structure and height of the auroras

The main information on auroral characteristics was obtained from the ASC films recorded at KEV and MUO. Both cameras are in a favourable position for estimating auroral altitudes and for locating the spatial distribution of the auroral structures within the field of view of the geophysical network. The method is described in detail in Kaila (1981). ASC information from MMK (Loparskaya) is used to obtain auroral data from the eastern sector (113°–125° CG Long), where the footpoint of the IMP-J satellite was located. Unfortunately, the temporal resolution of the ASC data (1 frame/min) is not high enough to study details of the auroral responses to the impulses. Hence the main interest will lie in comparing the location of the bright, active auroras with that of the vortices. The original ASC pictures from KEV in Fig. 5 give an impression of the variations in auroral brightness and structures while more quantitative information on auroral location and lower-border altitude is given in Fig. 6.

The auroral activity in Fig. 5 can be divided into four stages:

1959–2002 UT: The first sign of the auroral break-up was observed at 1959:03 UT as an inhomogeneous brightening (ripples) of the most equatorward arc within the 108°–115° CG longitudinal sector. This observation is confirmed by the SMA magnetometer data with a 10-s time resolution. Thereafter the auroras brighten rapidly and the

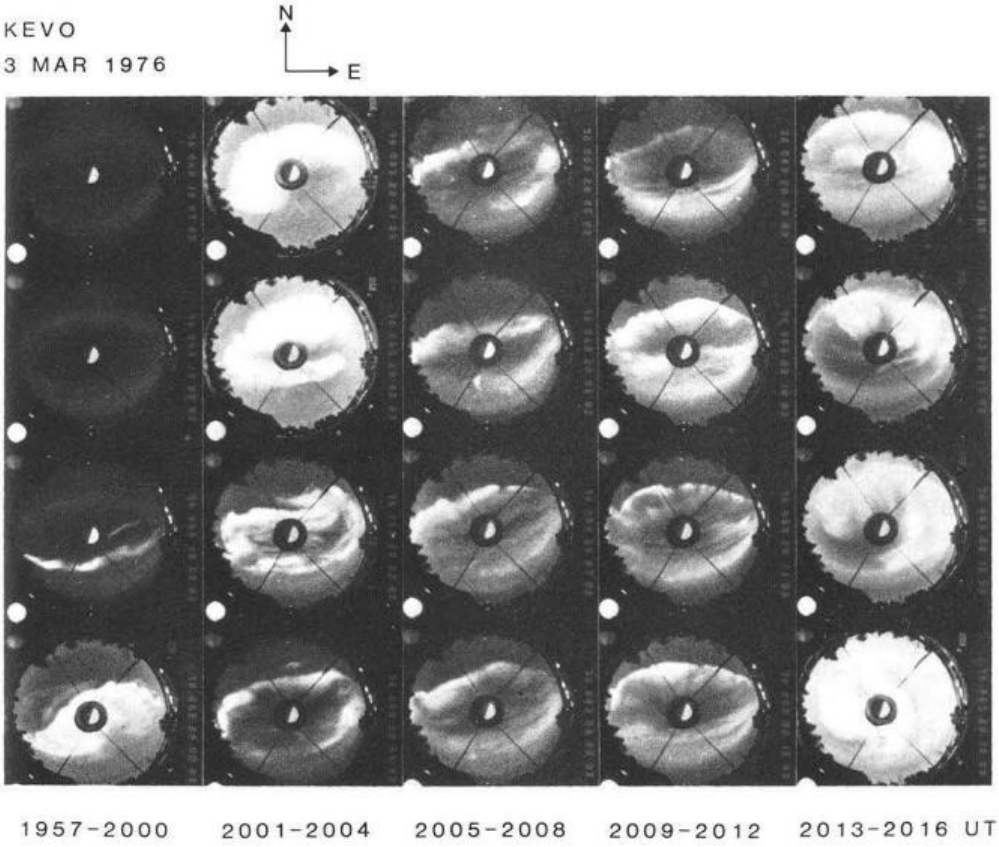

Fig. 5. All-sky camera data recorded at Muonio from 1957 to 2016 UT

bulge is formed at 2000 UT within the sector 110°–118° CG Long. The westward-travelling surge (WTS) on the western edge of the bulge coincides in space with the vortex structure A in Fig. 4. One more important detail is the thin bright structure appearing at 2002 UT in the eastern poleward half of the bulge (Fig. 5). According to the simultaneous ASC data from Loparskaya, the active structure expanded eastwards as far as 120°–125° CG Long. This eastward expansion, taking place after A′, agrees well with the increase in the magnetic *A* component observed only at LOZ in Fig. 3.

2003–2008 UT: The most significant difference compared with the previous interval is the fading of auroral activity over Kevo, while the activity seems to continue in the west (data not shown). This is in good agreement with the location of the vortices and CNA peaks at the moments B and D in Figs. 3 and 4. The westward expansion continues at an average speed ~2°/min.

The magnetic *A* component at MUO (Fig. 3) shows an impulsive rise starting at 2003 (B) and leading to the formation of vortex B in Fig. 4. At the same time the ASC picture from MUO (data not shown) reveals a rippled structure (inhomogeneous brightening) ahead of the WTS, in a place where the WTS is located 1 min later. This development closely resembles that observed at the initial break-up. The rippled structure appearing abruptly in a previously undisturbed region may be regarded as a sign of auroral response to the onset of impulse.

2009–2012 UT: No clear impulsive signs in CNA (the CNA onset at KEVO marked by a triangle in Fig. 3 occurred well before 2009 UT), Pi2 or equivalent currents are evident during this period. The brightening of the bulge at 2010 (Fig. 5) is associated with a spike (E) in the Pi1B data (Fig. 2a). No significant changes in auroral structure, location or height are recorded (Fig. 6). Some weak continuous poleward expansion is observed along the western meridian.

2013–2016 UT: The auroras brighten rapidly and expand both equatorwards and polewards, as seen at Kevo (Fig. 5). The most effective poleward movement, associated with impulse G, takes place along 113° CG Long between 2014 and 2017 UT (Fig. 6). After 2017 the edge of the bulge is seen at such low elevation angles (10°–15°) that only limited information on auroral variations can be obtained. A sudden intensification at 2023 UT (data not shown) can be detected within 105°–115° CG Long and ~70°–71° CG Lat, obviously associated with impulse I (Fig. 3) and the CNA enhancement at BJN (Fig. 1).

The auroral observations presented above seem to agree with the material presented in the previous sections. A close correlation both in strength and location was found between auroral activity and impulsive vortex formation. When the response in vortex formation was extremely weak (cf. impulse E) no deformation in auroral structures or changes in height were observed during a clear auroral brightening. Still, this comparison must nevertheless be considered incomplete due to inadequate time resolution.

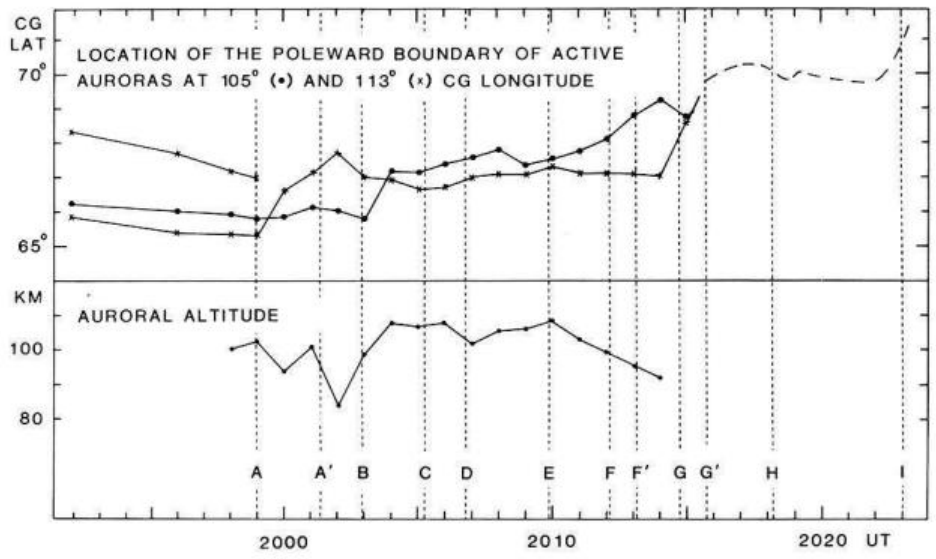

Fig. 6. Position of the poleward boundary of active auroral structures (bright edge of the auroral bulge after break-up) obtained from digitized ASC films from Muonio and Kevo (*top panel*). Altitude variations of the bulge edge obtained by triangulation (*bottom panel*). A rough estimate of the auroral development after 2016 UT is indicated by the *broken line*

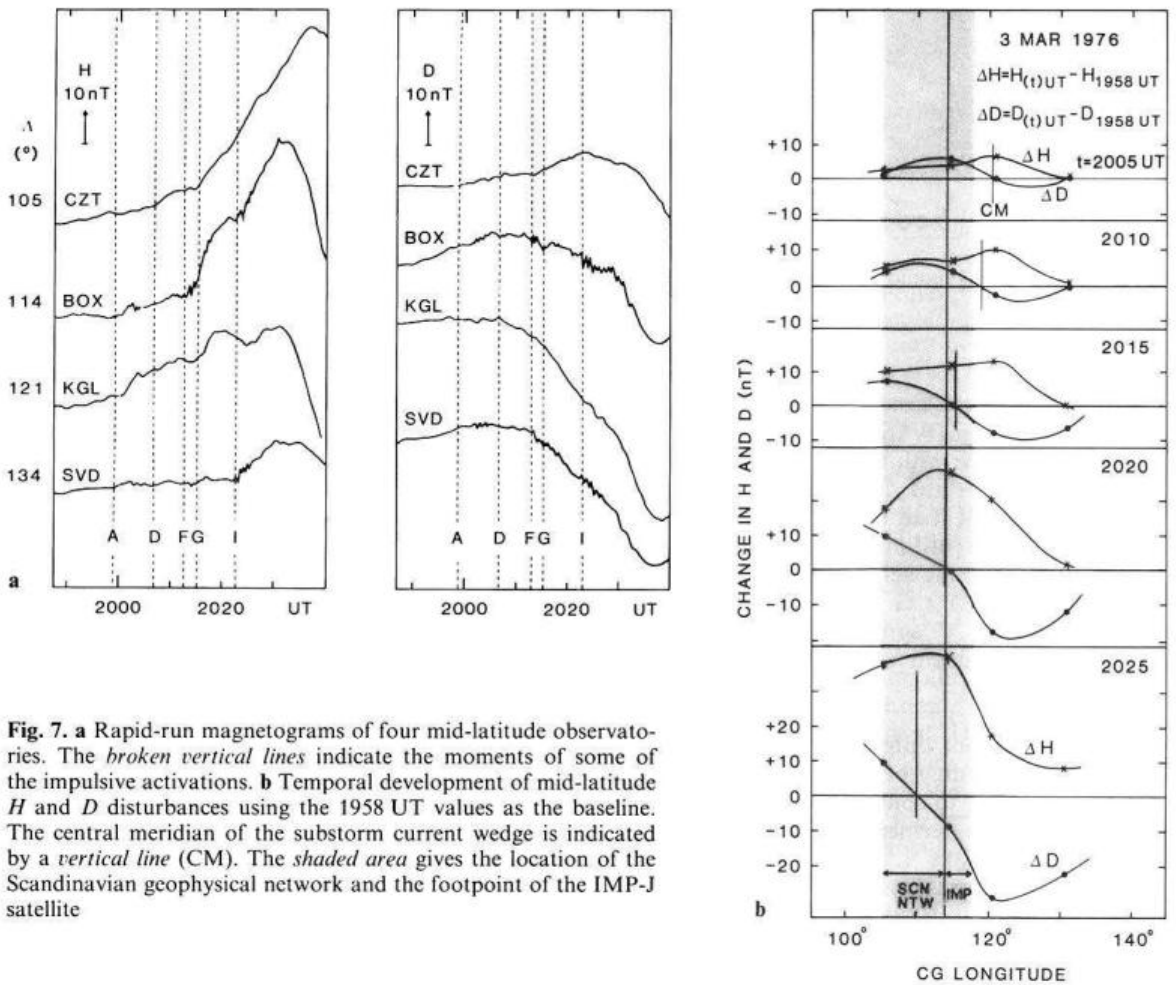

Fig. 7. a Rapid-run magnetograms of four mid-latitude observatories. The *broken vertical lines* indicate the moments of some of the impulsive activations. **b** Temporal development of mid-latitude *H* and *D* disturbances using the 1958 UT values as the baseline. The central meridian of the substorm current wedge is indicated by a *vertical line* (CM). The *shaded area* gives the location of the Scandinavian geophysical network and the footpoint of the IMP-J satellite

Three-dimensional substorm current wedge

Variations in the intensity and position of the expansion-related three-dimensional substorm current wedge (SCW) system were monitored by four stations located along 52°–58° CG Lat within 105°–134° CG Long (Fig. 7a). Two of these, CZT and KGL, located in the southern hemisphere, provided digital data with 1-min time resolution, while rapid-run (90 mm/h) sensitive magnetograms were available from BOX and SVD in the northern hemisphere. No significant qualitative differences in SCW behaviour were found between hemispheres. The effects in terms of

both auroral electrojet and field-aligned currents (FAC) are larger at KGL, located at 58.5° CG Lat, 5°–6° poleward of the other stations than at the lower-latitude stations. This has to be taken into account in the data analysis, especially when presenting longitudinal profiles (Fig. 7b).

The changes in the horizontal magnetic field after the onset of the substorm at mid-latitudes (Fig. 7b) are typical of a SCW system. The ΔD profile resembles a sinusoidal wave in which D changes its sign at the variation maximum ΔH. This point may be regarded as the central meridian of the SCW system. According to McPherron et al. (1973), the maximum and minimum for ΔD should be located at meridians in which the FACs are directed into the ionosphere or out of it, respectively.

At the onset (A), the H-component increase at BOX and KGL and the D-component increase at BOX and CZT indicate the appearance of the SCW around 115°–120° CG Long, in good agreement with other data. At 2007 (D) H starts to increase more rapidly at CZT and D decreases at KGL, indicating a westward expansion of the SCW. The whole pattern shifts westwards and intensifies during impulses F, G and H, and finally, at impulse I, a new intensification of the SCW starts, expanding eastwards (rise in H at SVD) and westwards (decrease in D at CZT). Comparison of the pattern of the SCW system with the vortex positions in Fig. 4 leads us to conclude that all the vortices appear in the western part of the SCW and are highly localized compared with the total size of the SCW (Fig. 7b).

The intensity of the SCW increases throughout the period studied here, but the rate of increase and the spatial configuration clearly change in response to major intensifications in currents and precipitation in the auroral zone. There also seems to be a close relationship between SCW intensifications and the poleward expansion of auroras (Fig. 6). Hence, the SCW system seems to integrate the effects of individual impulses, leading to long time constants (up to 20–30 min).

IMP-J observations and their relation to ground phenomena

In the following we will refer to the magnetic field and energetic particle data presented in Fig. 3 of paper I. As can be seen from this figure, the magnetic field increased up to the data gap, which started at 2025 UT. The thermal electron energy density decreased during this time interval with the exception of a brief partial recovery between 2007 and 2015 UT (E.W. Hones, personal communication). After the onset at 1959 UT, high fluxes of accelerated HE particles (especially electrons) appeared. The proton fluxes were highly anisotropic with a pronounced tailward flow component until the end of the interval considered. The HE electrons had practically isotropic pitch-angle distributions, and it was only during two brief intervals (at 2018 and 2023 UT) that the 30-keV electron fluxes showed any pronounced tailward anisotropy (ratio >2). The significance of these observations will be discussed later.

In order to compare the IMP-J satellite data with ground recordings, the ionospheric projection of the magnetic field line passing through the satellite has been estimated using different variants of the magnetospheric model of Tsyganenko (1979), which takes into account the tilt of the dipole axis and the shift in the position of the neutral sheet. The different variants give large variations in projected latitude, but the longitude remains fairly constant (within a few degrees) around 117° CG Long. Hence it seems safe to pay principal attention to the longitudinal effects when comparing satellite recordings with ground data. It is evident that even the longitude can be severely distorted by the SCW system, but not in our case since the projection point is close to the SCW central meridian (Fig. 7b), where longitudinal distortions are minimal (Vasyliev et al., 1986).

As can be seen in Fig. 3 of paper I, short-lived HE particle spikes with an enhancement of more than an order of magnitude are recorded in both the e^- and p^+ components during activation A–A′, F–F′, G–G′ and J (the primed letters are taken from the corresponding figures of this paper, paper II). The rise in particle fluxes after 2007 UT looks different and may be associated with the partial recovery of the PS seen in the thermal plasma data. One more spike appears at 2010 UT (E), which is recorded most clearly in the electron channel.

A detailed comparison of ground and satellite recordings reveals that spikes A, F′ and G appear in conjunction with short-lived vortex structures (Fig. 4) developing near the satellite conjugate point in the eastern part of the ground-based network. There was no vortex formation during impulse E, but the aurora was also activated in this sector. Both the auroral and CNA observations at moment I indicate that this event was centred over Bear Island, at 110° CG Long. HE particle spikes do not appear at moments B, C, D and H, when there was intense vortex formation only 5°–10° to the west of the easternmost vortices. The vortex formations were associated with local enhancements in CNA, indicating peak precipitation of HE particles at their centres, as in the case of the easternmost vortices. It may be concluded from these observations that the main acceleration region in the PS was shifted with respect to the IMP-J position. A shift of 5°–10° in the peak precipitation region in the ionosphere corresponds to only about 2 R_E shift across the tail at $x \simeq 20$–40 R_E. In practice, this means that the acceleration region is fairly localized and very small in size.

Discussion

Impulsive structure as a common feature of substorms and their relationship to microsubstorms

We shall discuss initially to what extent this event is a representative example of substorm expansion. At first glance, there seem to be some uncommon features: the continuously growing, large (compared with the expansion-related disturbances in Figs. 1 and 3) convection-related auroral electrojet, the spatially confined active region and the unusually rich impulsive fine structure (it is quite rare to find more than ten distinct Pi1B impulses in a single-station sonagram).

A detailed study of the literature reveals, however, that these features are not so uncommon. Strong (or growing) twin-vortex current systems appear in practice during all substorms that occur in conjunction with continuously southward-directed IMF. This has been clearly demonstrated in studies where the global twin-vortex current system and the expansion-related current pattern have been separated (Troshichev et al., 1974; Baumjohann et al.,

1981). According to these authors (see also Pellinen et al., 1982; Yahnin et al., 1983; Kamide and Baumjohann, 1985), the relative strength of these two current systems varies in a wide range from case to case, the twin-vortex current system being mainly controlled by the IMF variations. A similar type of control is also evident for changes in the magnetic field of the tail lobes (Fairfield et al., 1981).

In most substorm studies so far the authors have preferred to select well-isolated cases associated with an abrupt, strong negative magnetic bay in the nightside auroral zone. Such cases are more rare than those characterized by the magnetograms in Fig. 1. The choice of such uncommon cases also predetermines the properties of substorms to be observed. In such cases it is typical for the active part of the auroral bulge to move quickly away from the initial break-up region, thus preventing one-site observations of a large number of impulsive activations associated with bulge formation. Such activations have been well-documented in cases having a small-scale, moderate-intensity auroral bulge (Bösinger et al., 1981; Yahnin et al., 1983, 1984). Hence the relatively small dimension of the active region in our case and the consequent rich impulsive activity are due to the relatively weak expansion-related three-dimensional current system.

Microsubstorms are a common feature of substorm development and can be detected in magnetograms with ordinary time resolution, as in Fig. 1. The results presented here show the microsubstorms (I, II and III in Fig. 1) to consist of groups of distinct impulses. The first started within 110°–120° CG Long (A, A′) with the vortices associated with the following impulses (B, C, D) observed further west. A similar spatial development in vortex position was found in the second microsubstorm (F, G, H) and possibly in the third one, where the activity was again initiated in the same sector, shifting westwards later. It may be speculated that a microsubstorm is not a simple superposition of impulses, but also includes some rules controlling their spatial development. It is possible that control of the repetition rate, strength and position of the impulses is due to some (unknown) feedback in the magnetosphere-ionosphere system.

Impulsive activations have been found in all recordings made with appropriate time resolution under the active part of an auroral bulge. Balloon-borne X-ray recordings were the first to be reported in the literature (Hones et al., 1971; Pytte et al., 1976b; Melnikov et al., 1976). A close relationship between X-ray bursts, Pi1 bursts and the appearance of short-lived current vortices has been demonstrated by Yahnin et al. (1983) and the coincidence of current vortex and Pi1B appearance by Bösinger et al. (1981). It has been shown that all these impulsive features can be recorded simultaneously only in an extremely limited area of the auroral zone, under the active part of the expanding auroral bulge. A similar type of restriction is also valid for observations made in the magnetotail. The changes of recording impulsive bursts are strongly dependent on the shift of the small-sized source in a cross-tail direction (see later) and on the position of the satellite in relation to the outer boundary of the PS, which changes rapidly in the course of a substorm. In our case and in those presented by Sergeev et al. (1978, 1981) multiple bursts seem to appear near the dynamic boundary of the PS.

The sudden changes in the characteristics of Pi2 pulsations observed at mid-latitudes (Fig. 2b) are closely related to the impulsive phenomena observed in the auroral zone and magnetotail (Sergeev et al., 1978; Sergeev, 1981; Yahnin et al., 1983). Use of the mid-latitude Pi2 *alone* as a (quantitative) indicator of impulsive activity in the auroral zone is somewhat dangerous, however, as in most cases it permits one to infer the number of impulsive activations regardless of their strength and size in the auroral zone (see also Yahnin et al., 1983). This strongly supports the idea that all substorms develop through brief impulsive activations of a common nature.

Three-dimensional substorm current wedge

The formation of a substorm current wedge is due to an interaction between the ionosphere and the magnetosphere. We have demonstrated here that the growth in its intensity and spatial extent is intimately related to the strongest impulses associated with spikes in HE electron precipitation, rapid auroral expansions and the formation of current vortices. In addition to the impulsive changes, there is a continuous increase in the SCW intensity during the entire period studied. The smooth character of the mid-latitude magnetic bays (Pi2s subtracted) is an indicator of a long time constant (of the order of 20–30 min) for the SCW system, probably due to the high inductance of such an electric circuit (Boström, 1974).

How do the impulsive activations produce or control the SCW? The answer is not clear. An impulsive dissipative process in the plasma sheet launches Alfvén waves propagating both earthwards and tailwards, away from the source region. The earthward wavefront carries a westward current closed by field-aligned currents directed into (out of) the ionosphere at the eastern (western) edge of the disturbance (paper I; Hill and Reiff, 1980). Similar current configurations have been found in a numerical simulation study of tail reconnection by Sato et al. (1983).

Enhanced precipitation into the ionosphere will produce a similar FAC configuration (Baker et al., 1984) and will launch a corresponding Alfvén wave into the magnetosphere (Maltsev et al., 1974). The relative importance and interaction of the two mutually acting processes in generating the SCW are unexplored at present.

The existence of a SCW can influence both the PS and auroral-zone dynamics. A continuous growth in SCW intensity leads to an enhanced electric field in the PS (~ 1 mVm^{-1}; Semenov and Sergeev, 1981). A SCW creates magnetic-field deformation, which moves the auroras poleward (Akasofu, 1977) and apparently forms the auroral bulge (Vasyliev et al., 1986). Hence, both poleward and westward expansions superimposed on the impulse-related changes are to be expected during continuous growth of the SCW. In our case, westward motion was observed until 2010 UT, when the structure moved beyond the field of view of our all-sky cameras.

Impulse-induced phenomena: spatial extent and intensity correlation

A counterclockwise differential equivalent current vortex seems to be a common feature of substorm expansion. The vortices are typically short-lived (~ 5 min) and appear at different places during different stages of expansion. They

are superimposed on a smooth, large-scale (convective) current system, as shown by Baumjohann et al. (1981). Yahnin et al. (1983) demonstrate that Pi1Bs, X-ray bursts, CNA impulses in the auroral zone and Pi2s at mid-latitudes appear simultaneously with current vortices. The results presented here are similar, but extend the observations to a later stage, beyond the first few minutes of the expansion phase.

Magnetic-field topology in the boundary-layer plasma sheet, as inferred from the dawn-dusk asymmetry of the high-energy particle fluxes

A few striking features can ce observed in the long-term development of the thermal PS population and the HE particle fluxes (Fig. 3, paper I). Fluxes of thermal plasma decrease significantly, except for the short partial recovery between 2007 and 2015 UT, and the HE proton fluxes show similar behaviour. The HE electron fluxes are surprisingly steady and high (well above their pre-onset values), especially at higher energies. In order to understand the high flux of very hot electrons in the PS boundary layer, the following has to be pointed out:

There is an almost isotropic pitch-angle distribution of high-energy electrons between the short bursts, which suggests magnetic trapping. Hence, the magnetic field lines penetrating the PS boundary layer must be closed (connected to the ionosphere or closed field line loops). The observed proton-electron asymmetry can be explained as being due to the spatial separation between the satellite and the acceleration region in the cross-tail direction (cf. paper I). When this region is west of IMP-J, accelerated electrons that drift eastwards in the PS magnetic field appear at the satellite. This is in agreement with our ground observations, since the vortex structure always appeared westwards of the satellite footpoint. These observations support the conclusion that the cross-tail extent of the acceleration region is very limited and that the magnetic flux tube connected to the vortex structure passes near the acceleration region in the far PS.

Figure 8 presents some limited statistics to support the above conclusion. The IMP-J made observations of strong substorm expansions (AE > 500 nT) in the PS on six occasions. The first five are from 3 March 1976, 1000 to 2400 UT, and the last one from 20 February 1976, as studied earlier by Krimigis and Sarris (1979). Data from two proton and electron channels in the CPME experiment are plotted. The arrows on the top indicate onset times of mid-latitude Pi2s and Pi1Bs in the auroral zone in the 2200–0000 MLT time sector. The onsets of irregular pulsations seem to occur simultaneously with HE particle spikes (within 1 min). Some differences between the Pi1B and Pi2 moments exist, but these cannot be studied due to the limited station coverage in the active sector of the auroral zone. The events in Fig. 8 are ordered according to the Y_{GSM} coordinate of IMP-J. In the westernmost position (a) the protons develop a spike, while in the easternmost location (e, f) the electrons show the most distinct increases. This demonstrates that over a relatively limited cross-tail distance ($\sim 8\ R_E$) there is a significant electron-proton asymmetry in the response to substorm onsets. Also, the acceleration region seems to be displaced into the duskward half of the PS. This observation is in agreement with the results of Krimigis and Sarris (1979), where the frequency

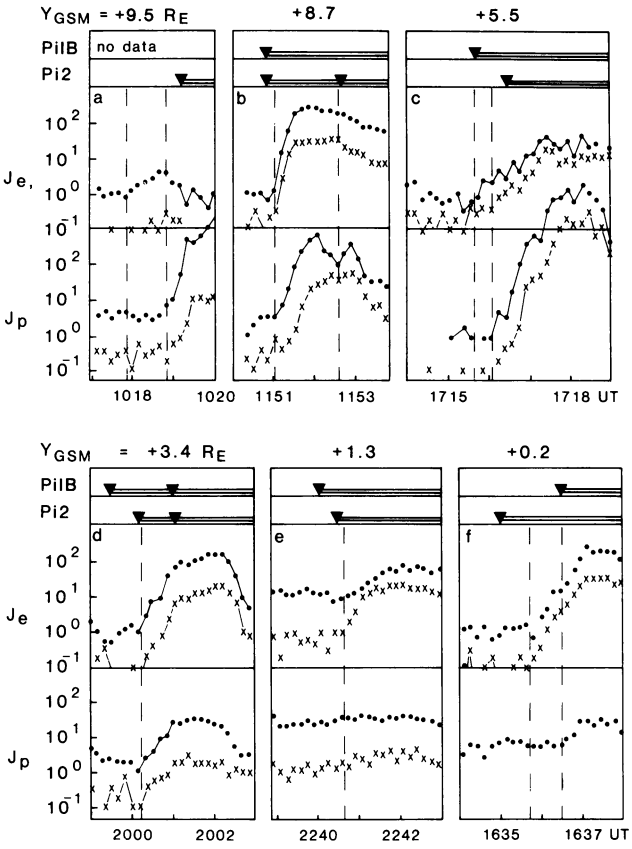

Fig. 8. Electron and proton count rates from two high-energy channels recorded by IMP-J during six strong substorm expansions (AE > 500 nT). The *Y* position of the satellite is given on the top ($x < -35\ R_E$). The onset times of mid-latitude Pi2s and Pi1Bs in the auroral zone are indicated by the *arrows and broken vertical lines*

of occurrence of HE particle bursts was studied under similar conditions.

The proposed loop-type configuration of magnetic field lines tailward of the particle acceleration region is consistent with the "neutral line model" of Hones (1979), where the field lines beyond the neutral line are stretched into the far tail and closed across the equator tailward of the escaping plasmoid. According to recent ISEE-3 observations reported by Hones et al. (1984), a plasmoid reaches $x \sim -200\ R_E$ some 20–30 min after the onset of a substorm, which means in our case that the length of the magnetic loop will be a few hundred R_E after an expansion phase of 25 min. Such a length partially explains both the almost isotropic pitch-angle distribution of the HE electrons between the brief bursts and the strong tailward anisotropy during some bursts. HE electrons travelling with a speed of $> 10\ R_E/s$ take about 1 min to travel around the loop. Hence, during the first half-minute interval (when the acceleration power is increasing impulsively) the electrons are streaming mainly tailward, while during the second half (when the acceleration ceases) the anisotropy fades due to the returning electrons and their pitch-angle diffusion. The length of the magnetic loop depends on many parameters: e.g. the stage of expansion (i.e. the position of the plasmoid) and the amount of magnetic flux developed in the PS region during the pre-substorm condition.

Cross-tail extent of the acceleration region

HE particle observations made simultaneously by two spacecraft led Krimigis and Sarris (1979) to suggest that the extent of the acceleration region in the Y direction is only a few R_E ($<10\ R_E$). As far as we know, there are no other published results dealing with this important parameter. Moreover, the same authors claim that observed HE particle bursts are sensitive to the Z coordinate of the spacecraft. This means that their conclusions should be approached with a certain degree of care, although our results are in compliance with their view.

The asymmetry of the HE protons and electrons in the dawn-dusk direction in Fig. 8 suggests an extent of $<8\ R_E$ for the acceleration region (i.e. <20% of the total tail width). According to the various magnetospheric models (e.g. Tsyganenko, 1979) 1 h in MLT (15° in longitude) in the nightside auroral oval corresponds to a width of 3–4 R_E at $x\sim-15\ R_E$. At 2001–2002 (i.e. towards the end of the first HE particle burst) the active auroras were confined between 108° and 120° CG Long, but a few minutes later at 2005 UT the width of the SCW was between 10° and 20° CG Long. In any case, the longitudinal width of the active region at the onset of the substorm was <30° (=2 h MLT), which means that the value $\Delta Y=8\ R_E$ serves well to characterize the upper limit of the dawn-dusk extent of the active region in the magnetotail.

Errors in magnetic projection between the equatorial magnetotail and the ionosphere are to be expected, due to deformation of the magnetic field in the PS during substorms. The relative displacement of the active regions in the ionosphere and its influence on the appearance of HE particle bursts at the satellite nevertheless allow us to draw some conclusions on the size of the active region in the Y direction. HE particle bursts are recorded at the satellite during the "eastern" cases in Fig. 4 (vortex centre within 10° CG Long of the estimated satellite projection meridian), while a 5°–10° CG Long westward shift of the vortex seems to prevent these observations. This sets the lower limit of the size of the acceleration region at $\Delta Y\sim2$–$3\ R_E$.

Impulse-related disturbances in the magnetic field and thermal plasma may appear more widely in the magnetotail due to different propagation modes, e.g. magnetosonic and magnetohydrodynamic waves. Long-term enhancements in HE particle fluxes due to drift and diffusion (like the observations after 2007 UT in our case) are also observed. Hence, brief field-aligned HE particle bursts are the most important tracers of the source region, since particles accelerated at source appear immediately on the magnetic field lines connected to the source.

According the theoretical model of Pellinen and Heikkila (1984), and more recently that of Zeleny et al. (1984), the inductive electric field in the proximity of the X-type neutral line and within the magnetic loop produces the observed characteristics of the HE particle bursts. The mechanism may be a non-linear (explosive) tearing process (Galeev, 1982), an assumption which would predict both the duration of the HE particle burst and the ΔY size of the acceleration region (5–10 R_E).

Conclusions

1. The present study of a dozen impulsive activations occurring during the first 25 min of a substorm in an approximately constant MLT sector enables us to extract information on the ground-based patterns associated with both short-lived (1–3 min) and longer-term variations.

2. The short-lived patterns appearing in the auroral zone during the impulsive activations are counterclockwise rotating differential equivalent current (vortex), enhancement in the CNA within the vortex and brightening and/or deformation of auroral structures in the same area. The appearance of the vortex is associated with Pi1B-type pulsations in the auroral zone and a change in Pi2 characteristics at mid-latitudes. The time constant of the vortex is 2–3 min and its diameter about 400 km.

3. Impulsive spikes of HE protons and electrons ($E>$ 0.2 MeV) are observed in the far magnetotail (37 R_E) only in cases where the meridional projection of the satellite is near the vortex. Asymmetry in the occurrence of HE protons and electrons is observed within only 8 R_E across the tail. Our estimates give 2–8 R_E for the ΔY dimension of the acceleration region.

4. Stable signatures of closed magnetic field lines are observed within 25 min of the onset of the substorm in the plasma sheet boundary layer at 37 R_E, well beyond the major acceleration region (X-type neutral line).

5. The substorm current wedge seems to integrate the effects of the elementary impulses. This leads to a longer time constant for the SCW (>10 min). The vortex formation and HE particle precipitation events jump between locations within the western part of the SCW.

6. A microsubstorm consists of several elementary impulses and is modulated by their intensity and spatial displacement.

Acknowledgements. IMP-J recordings of magnetic fields (Drs. N.F. Ness and R.P. Lepping, principal investigators) and energetic particles (Dr. D.J. Williams, principal investigator of the EPD experiment) were obtained through WDC-A (Rockets and Satellites) by courtesy of Dr. J.I. Vette. Digital magnetic field data from the Port Alfred and Kerguelen observatories were provided by WDC-A (geomagnetism). Other ground magnetic field data were obtained through WDC-B in Moscow. The riometer data from Finland were provided by the Sodankylä Geophysical Observatory. We are grateful to Drs. G.A. Loginov, Ya.M. Gogatishwili, B.I. Klain and L.N. Ivanova for allowing us to use their rapid-run and induction magnetometer recordings, and to all the colleagues who participated in the collection of the data for 3 March 1976. The SMA observations and the work of W. Baumjohann were supported financially by grants from the Deutsche Forschungsgemeinschaft. The work by V. Sergeev, R. Pellinen and T. Bösinger was supported by the Finnish-Soviet Committee on co-operation in science and technology.

References

Aggson, T.L., Heppner, J.P.: Observations of large transient magnetospheric electric fields. J. Geophys. Res. **82**, 5155–5164, 1977

Akasofu, S.-I.: Polar and magnetospheric substorms. Dordrecht: D. Reidel, 1968

Akasofu, S.-I.: Physics of magnetospheric substorms. Dordrecht: D. Reidel 1977

Baker, D.N., Akasofu, S.-I., Baumjohann, W., Bieber, J.M., Fairfield, D.H., Hones, E.W., McPherron, R.L., Moore, T.E.: Substorms in the magnetosphere. Chapter 8, Solar-terrestrial physics – present and future. K. Papadopoulos and D. Butler, eds. NASA, Washington, D.C., 1984

Baumjohann, W., Mishin, V.M., Saifudinova, T.I., Shpynev, G.B., Bazarzhapov, A.D.: Substorms, microsubstorms and disruption of currents in the magnetospheric plasma sheet. Issled. Geomagn. Aeron. Fys. Sol. (in Russian), **53**, 182–191, 1981

Boström, R.: Ionosphere-magnetosphere coupling. In: Magnetospheric physics, M. McCormack, ed.: pp. 45–59. Dordrecht: D. Reidel 1974

Bösinger, T., Alanko, K., Kangas, J., Opgenoorth, H.I., Baumjohann, W.: Correlations between PiB type magnetic micropulsations, auroras and equivalent current structures during two isolated substorms. J. Atmos. Terr. Phys. **43**, 933–945, 1981

Coroniti, F.V., Frank, L.A., Williams, D.J., Lepping, R.P., Scarf, F.L., Krimigis, S.M., Gloeckler, G.: Variability of plasma sheet dynamics. J. Geophys. Res. **85**, 2957–2977, 1980

Fairfield, D.H., Lepping, R.P., Hones, E.W., Bame, S.I., Asbridge, J.R.: Simultaneous measurements of magnetotail dynamics by IMP spacecrafts. J. Geophys. Res. **86**, 1396–1414, 1981

Galeev, A.A.: Magnetospheric tail dynamics. In: Magnetospheric plasma physics. A. Nishida, ed.: p. 143. Center for Academic Publ. Japan, 1982

Hill, T.W., Reiff, P.H.: Plasma sheet dynamics and magnetospheric substorms. Planet. Space Sci. **28**, 363–374, 1980

Hones, E.W.: Plasma flow in the magnetotail and its implications for substorm theories. In: Dynamics of the magnetosphere. S.-I. Akasofu, ed.: pp. 545–562. Dordrecht: D. Reidel 1979

Hones, E.W., Karas, R.H., Lanzerotti, L.I., Akasofu, S.-I.: Magnetospheric substorms on September 14, 1968. J. Geophys. Res. **76**, 6765–6780, 1971

Hones, E.W., Baker, D.N., Bame, S.J., Feldman, W.C., Gosling, J.T., McComas, D.J., Zwickl, R.D., Slavin, J.A., Smith, E.J., Tsurutani, B.T.: Structure of the magnetotail at 220 R_E and its response to geomagnetic activity. Geophys. Res. Lett. **11**, 5–7, 1984

Kaila, K.U.: Three-dimensional mapping of the aurora from digitized all-sky pictures. Finn. Met. Inst., Technical Report No. 25, 38, 1981

Kamide, Y., Baumjohann, W.: Estimation of electric fields and currents from IMS magnetometer data for the CDAW-6 intervals: Implications for substorm dynamics. J. Geophys. Res. **90**, 1305–1317, 1985

Krimigis, S.M., Sarris, F.T.: Energetic particle bursts in the Earth's magnetotail. In: Dynamics of the magnetosphere, S.-I. Akasofu, ed: pp. 599–630. Dordrecht: D. Reidel 1979

Küppers, F., Untiedt, J., Baumjohann, W., Lange, K., Jones, A.G.: A two-dimensional magnetometer array for ground-based observations of auroral zone currents during IMS. J. Geophys. **46**, 429–450, 1979

Maltsev, Yu.P., Leontyev, S.V., Lyatsky, W.B.: Pi2 pulsations as a result of evolution of an Alfvén impulse originated in the ionosphere during a brightening of aurora. Planet. Space Sci. **22**, 1519–1533, 1974

McPherron, R.L., Russel, C.T., Aubry, M.P.: Satellite studies of magnetospheric substorms on August 15, 1968 (9). J. Geophys. Res. **78**, 3131–3147, 1973

Melnikov, A.O., Khrushinsky, A.A., Zhulin, I.A., Kornilov, I.A., Lazutin, L.L., Raspopov, O.M., Riedler, V.K., Sakharov, Ya.A., Tagirov, V.R., Treilhou, T.P.: X-ray burst structure of break-up and Pi2 geomagnetic pulsations. In: Dynamical processes and structure of auroral magnetosphere (SAMBO experiment) (in Russian). Ed. Kola Branch Acad. Sci. USSR, pp. 28–42, Apatity 1976

Mishin, V.M., Nemtsova, E.I., Saifudinova, T.I., Urbanovich, V.D., Loginov, G.A., Sergeev, V.A., Danilov, A.A., Sobolev, A.V., Solovjev, S.I., Zaitsev, A.N., Lyubimova, N.P., Shevnina, N.F., Baumjohann, W.: Results of observations during substorms on March 3, 1976. 2. Data of geomagnetic observations. Preprint SibIZMIR N1–82, Irkutsk, 1982

Opgenoorth, H.I., Pellinen, R.J., Maurer, H., Küppers, F., Heikkila, W.J., Kaila, K.U., Tanskanen, P.: Ground-based observations of an onset of localized field-aligned currents during auroral break-up around magnetic midnight. J. Geophys. **48**, 101–115, 1980

Pellinen, R., Heikkila, W.J.: Inductive electric fields in the magnetotail and their relation to auroral and substorm phenomena. Space Sci. Rev. **37**, 1–61, 1984

Pellinen, R.J., Baumjohann, W., Heikkila, W.J., Sergeev, V.A., Yahnin, A.G., Marklund, G., Melnikov, A.O.: Event study on pre-substorm phases and their relation to the energy coupling between solar wind and magnetosphere. Planet. Space Sci. **30**, 371–388, 1982

Pytte, T., McPherron, R.L., Kivelson, M.G., West, H.I., Hones, E.W.: Multiple-satellite studies of magnetospheric substorm. Radial dynamics of the plasma sheet. J. Geophys. Res. **81**, 5921–5933, 1976a

Pytte, T., Trefall, H., Kremser, G., Tanskanen, P., Riedler, W.: On the morphology of energetic (>30 keV) electron precipitation at the onset of negative magnetic bays. J. Atmos. Terr. Phys. **38**, 757–773, 1976b

Pytte, T., McPherron, R.L., Kokubun, S.: The ground signatures of the expansion phase during multiple-onset substorms. Planet. Space Sci. **24**, 1115–1132, 1976c

Pytte, T., McPherron, R.L., Kivelson, M.G., West, H.I., Hones, E.W.: Multiple-satellite studies of magnetospheric substorms: Plasma sheet recovery and the poleward leap of auroral activity. J. Geophys. Res. **83**, 5256–5268, 1978

Ranta, H., Ranta, A., Collis, P.N., Hargreaves, J.K.: Development of the auroral absorption substorm: Studies of pre-onset phase and sharp onset using an extensive riometer network. Planet. Space Sci. **29**, 1287–1313, 1981

Rostoker, G., Akasofu, S.-I., Foster, J., Greenwald, R.A., Kamide, Y., Kawasaki, K., Lui, A.T.Y., McPherron, R.L., Russell, C.T.: Magnetospheric Substorms-Definition and Signatures. J. Geophys. Res. **85**, 1663–1668, 1980

Sato, T., Hayashi, T., Walker, R.J., Ashour-Abdalla, M.: Neutral sheet current interruption and field-aligned current generation by three-dimensional driven reconnection. Geophys. Res. Lett. **10**, 221–224, 1983

Semenov, V.S., Sergeev, V.A.: A simple semi-empirical model for magnetospheric substorm. Planet. Space Sci. **29**, 271–281, 1981

Sergeev, V.A.: On the longitudinal localization of substorm active region and its changes during the substorm. Planet. Space Sci. **22**, 1341–1343, 1974

Sergeev, V.A.: On the state of magnetosphere during prolonged periods of southward oriented IMF. Phys. Solariterr., Potsdam N 5, 39–50, 1977

Sergeev, V.A.: High-time resolution correlation between the magnetic field behaviour at 37 R_E distance in the magnetotail plasma sheet and ground phenomena during substorm expansion phase. J. Geophys. **49**, 176–185, 1981

Sergeev, V.A., Yahnin, A.G.: The features of auroral bulge expansion. Planet. Space Sci. **27**, 1429–1444, 1979

Sergeev, V.A., Yahnin, A.G., Raspopov, O.M.: On the spatial-temporal structure of the expansive phase of microsubstorm. In: Dynamical processes and structure of auroral magnetosphere (in Russian). O.M. Raspopov, L.L. Lazutin, eds.: pp. 42–54. Apatity 1978

Sergeev, V.A., Yahnin, A.G., Gorely, K.I., Danielson, C., Pellinen, R.J., Samsonov, V.P., Urbanovich, V.D., Latov, Yu.O., Ranta, H., Stauning, P., Armstrong, T.P., Hones, E.W., Krimigis, S.M., Lepping, R.P., Ness, N.F.: Results of observations during substorms on March 3, 1976. 1. Auroral precipitation data and measurements in the magnetotail. Polar Geophysical Institute preprint PGI-81-1, Apatity 1981

Sergeev, V.A., Bösinger, T., Lui, A.T.Y.: Impulsive processes in the magnetotail during substorm expansion. J. Geophys., 1986 this issue.

Troshichev, O.A.,. Kuznetsov, B.M., Pudovkin, M.I.: The current systems of the magnetic substorm growth and expansion phases. Planet. Space Sci. **22**, 1403–1412, 1974

Tsyganenko, N.A.: The subroutines and tables for calculation of geomagnetic field. WDC-B report, Moscow 1979

Untiedt, J., Pellinen, R., Küppers, F., Opgenoorth, H.J., Pelster, W.D., Baumjohann, W., Ranta, H., Kangas, J., Chechowsky, P., Heikkila, W.J.: Observations of the initial development of an auroral and magnetic substorm at magnetic midnight. J. Geophys **45**, 41–65, 1978

Vasyliev, E.P., Malkov, M.V., Sergeev, V.A.: Three-dimensional effects of substorm current wedge. Geomagn. Aeronomy (in Russian) **26**, 114–119, 1986

Vorobjev, V.G., Rezhenov, B.V.: Progressive westward displacements of the region of the auroral substorm localization in conjunction with impulsive variations of the magnetic field. Inst. Ass. Geomag. Aeron. Bull. **34**, 441–449, 1973

Wiens, R.G., Rostoker, G.: Characteristics of the development of the westward electrojet during the expansive phase of the magnetospheric substorm. J. Geophys. Res. **30**, 2109–2128, 1975

Yahnin, A.G., Sergeev, V.A., Pellinen, R.J., Baumjohann, W., Kaila, K., Ranta, H., Kangas, J., Raspopov, O.M.: Substorm time sequence and microstructure on November 11, 1976. J. Geophys. **53**, 182–197, 1983

Yahnin, A.G., Sergeev, V.A., Ievenko, I.B., Solovjev, S.I., Rakhmatulin, R.: Characteristics of phenomena, accompanied by the local flares of discrete auroras. In: Magnetospheric Res. (in Russian) **5**, 93–110, 1984

Zeleny, L.M., Lipatov, A.S., Lominadze, D.G., Taktakishvili, A.L.: The dynamics of the energetic proton bursts in the course of the magnetic field topology reconstruction in the Earth's magnetotail. Planet. Space Sci. **32**, 313–324, 1984

Received July 23, 1985 / Revised June 5, 1986
Accepted July 21, 1986